Microfluidic platform for electrophysiological studies on Xenopus laevis oocytes under varying gravity levels

Schaffhauser, D F ; Andrini, O ; Ghezzi, C ; Forster, I C ; Franco-Obregón, A ; Egli, M ; Dittrich, P S

Abstract: Voltage clamp measurements reveal important insights into the activity of membrane ion channels. While conventional voltage clamp systems are available for laboratory studies, these instruments are generally unsuitable for more rugged operating environments. In this study, we present a non-invasive microfluidic voltage clamp system developed for the use under varying gravity levels. The core component is a multilayer microfluidic device that provides an immobilisation site for Xenopus laevis oocytes on an intermediate layer, and fluid and electrical connections from either side of the cell. The configuration that we term the asymmetrical transoocyte voltage clamp (ATOVC) also permits electrical access to the cytosol of the oocyte without physical introduction of electrodes by permeabilisation of a large region of the oocyte membrane so that a defined membrane patch can be voltage clamped. The constant low level air pressure applied to the oocyte ensures stable immobilisation, which is essential for keeping the leak resistance constant even under varying gravitational forces. The ease of oocyte mounting and immobilisation combined with the robustness and complete enclosure of the fluidics system allow the use of the ATOVC under extreme environmental conditions, without the need for intervention by a human operator. Results for oocytes over-expressing the epithelial sodium channel (ENaC) obtained under laboratory conditions as well as under conditions of micro- and hypergravity demonstrate the high reproducibility and stability of the ATOVC system under distinct mechanical scenarios.

DOI: https://doi.org/10.1039/c0lc00729c

Originally published at:
Schaffhauser, D F; Andrini, O; Ghezzi, C; Forster, I C; Franco-Obregón, A; Egli, M; Dittrich, P S (2011). Microfluidic platform for electrophysiological studies on Xenopus laevis oocytes under varying gravity levels. Lab on a Chip, 11(20):3471-3478.
DOI: https://doi.org/10.1039/c0lc00729c

RSC Publishing Lab on a Chip

Microfluidic platform for electrophysiological studies on Xenopus laevis oocytes under varying gravity levels

Journal:	*Lab on a Chip*
Manuscript ID:	LC-ART-12-2010-000729.R1
Article Type:	Paper
Date Submitted by the Author:	n/a

Complete List of Authors:	Schaffhauser, Daniel; ETH Zurich, Chemistry and Applied Biosciences Andrini, Olga; University of Zurich, Institute of Physiology and ZIHP Ghezzi, Chiara; University of Zurich, Institute of Physiology and ZIHP Forster, Ian; University of Zurich, Institute of Physiology and ZIHP Franco-Obregón, Alfredo; ETH Zurich, Space Biology Group Egli, Marcel; ETH Zurich, Space Biology Group Dittrich, Petra; ETH Zurich, Department of Chemistry and Applied Biosciences

Microfluidic platform for electrophysiological studies on *Xenopus laevis* oocytes under varying gravity levels†

Daniel F. Schaffhauser,[a] Olga Andrini,[b] Chiara Ghezzi,[b] Ian C. Forster,*[b] Alfredo Franco-Obregón,[c] Marcel Egli*[c] and Petra S. Dittrich*[a]

Received (in XXX, XXX) Xth XXXXXXXXX 200X, Accepted Xth XXXXXXXXX 200X
First published on the web Xth XXXXXXXXX 200X
DOI: 10.1039/b000000x

Voltage clamp measurements reveal important insights into the activity of membrane ion channels. While conventional voltage clamp systems are available for laboratory studies, these instruments are generally unsuitable for more rugged operating environments. In this study, we present a non-invasive microfluidic voltage clamp system developed for the use under varying gravity levels. The core component is a multilayer microfluidic device that provides an immobilisation site for *Xenopus laevis* oocytes on an intermediate layer, and fluid and electrical connections from either side of the cell. The configuration that we term the Asymmetrical Transoocyte Voltage Clamp (ATOVC) also permits electrical access to the cytosol of the oocyte without physical introduction of electrodes by permeabilisation of a large region of the oocyte membrane so that a defined membrane patch can be voltage clamped. The constant low level air pressure applied to the oocyte ensures stable immobilisation, which is essential for keeping the leak resistance constant even under varying gravitational forces. The ease of oocyte mounting and immobilisation combined with the robustness and complete enclosure of the fluidics system allow the use of the ATOVC under extreme environmental conditions, without the need for intervention by a human operator. Results for oocytes over-expressing the epithelial sodium channel (ENaC) obtained under laboratory conditions as well as under conditions of micro- and hypergravity demonstrate the high reproducibility and stability of the ATOVC system under distinct mechanical scenarios.

Introduction

The regulated movement of selected ion species through ion conducting channels in the plasma and intracellular membranes is essential for cell survival as well as cellular functions such as osmoregulation and intra- and intercellular signalling.[1] Disturbance to ion channel function undermines cell survival and may potentially manifest itself as a diseased state on the organismal level.[2] Ion channel function can be physiologically regulated by chemical, physical or mechanical gradients. The actions of chemical and pharmacological agents such as channel blockers and modulators of ion channel function have been well characterized and the underlying molecular mechanisms elucidated; in contrast, the role and influence of physical and mechanical stresses is less clear. Mechanical stimulation such as shear forces and mechanical strain is known to induce rearrangements of the cell's mechanotransductive apparatus, including the cytoskeleton, as well as the expression pattern of cell-regulatory proteins that in turn can modulate ion channel activity.[3, 4]

Previous studies have shown that gravitational force influences the activity of ion channels involved in cellular mechanotransduction.[5, 6] In this context, it has been shown that muscle cells are particularly vulnerable to reductions in gravitational force, ultimately leading to muscle atrophy in response to chronic exposure to a low gravity environment.[7, 8] Moreover, intracellular calcium, a ubiquitous cellular second messenger, is also responsive to gravitational force, which in turn, would modulate channel or pump activity.[9] Finally, some cation channels are both calcium conductive and mechanically-regulated, uniting both modalities of cellular response influenced by gravitational forces.[10] Given the importance of proper ion channel function for cell survival and metabolism, and the inherent difficulties of making electrophysiological recordings under conditions of altered gravitational force, we initiated a multidisciplinary collaboration with the aim of designing a stable and automated recording platform to reliably monitor the biophysical consequences of altered gravitational forces on ion channel activity.

Characterization of ion channels is usually performed by controlling the transmembrane potential and simultaneously measuring the resulting transmembrane current (voltage clamp). Laboratory-based voltage clamp systems commonly use glass microelectrodes (intracellular, or patch) to control the transmembrane voltage. These electrodes are fragile and require careful micromanipulation by the operator. Recently, the feasibility of planar electrodes manufactured from poly(dimethylsiloxane) (PDMS)[11, 12] or glass[13] has been successfully demonstrated, thereby providing a reliable and robust alternative to glass microelectrodes and, importantly, obviating the need for micromanipulation typically required for patch clamping. Moreover, a number of microfluidic chips for performing planar patch clamping under laboratory conditions has been developed recently.[14-17] Advances in automated electrophysiology have demonstrated that

reproducible recordings can be obtained without significant operator intervention.[18] Nevertheless, these devices are generally designed for operation under standard laboratory conditions, and are not suitable for remote operation in a physically demanding environment. On the other hand, specialised microfluidic devices have been realised for use under extreme environmental conditions such as the sea[19] or the Martian atmosphere.[20] The implementation and optimization of a voltage-clamp device for studies under varying gravity conditions is particularly challenging, since changes in gravity are associated with alterations of the mechanical environment with profound physiological consequences, be it on an aeroplane (e.g. during parabolic manoeuvres), sounding rocket, or in ground laboratory-based systems such as random position machines, 3D clinostats or centrifuges.

The core module of our system is a multilayer microfluidic chip that allows for stable positioning of a single cell (in our case, a *Xenopus laevis* oocyte) and accurate determination of the current passing across the entire cell membrane in response to an externally imposed transcellular electrical potential. Our design, which we term the asymmetrical transoocyte voltage clamp (ATOVC) is akin to the previously described loose macropatch voltage clamp[21, 22] and transoocyte voltage clamp (TOVC),[23] however in our system only a small, well-defined patch of the oocyte membrane is exposed to test solutions. This has two consequences: (i) it facilitates the fast exchange of fluids exposed to the membrane patch through the microperfusion layer of the device, yet only requires low solution volumes; (ii) by permeabilising the remainder of the cell membrane we can readily gain electrical access to the cell interior and achieve voltage clamping of the patch. The microfluidic device is made of PDMS and encapsulated in a PMMA assembly that comprises fluid, pressure and electronic connections. A similar design was previously described by Dahan et al.[14] but did not incorporate a fully enclosed cell recording chamber and fluidics. We now describe how this concept was specifically adapted and modified to satisfy our design criteria by incorporating a cell immobilisation feature and, moreover, by having a liquid- and airtight system.

To demonstrate the feasibility of our system, we have performed measurements on *Xenopus laevis* oocytes that heterologously expressed the amiloride-sensitive epithelial sodium channel (ENaC). This channel was chosen because of its high specificity, fast kinetics and documented sensitivity to mechanical stimuli.[3, 24, 25] The advantages of the oocyte expression system in the context of gravity research is that these cells are extremely robust and they can be easily transported, maintained and handled without requiring special incubation conditions or stringent sterility procedures. Moreover, after removal from the frog, they can be kept healthy for typically up to a week, provided the incubation temperature remains below 20 °C. A further unique feature of *Xenopus laevis* oocytes is that their orientation with respect to the Earth's gravitational field is well defined, with the easily identified animal pole (pigmented hemisphere) facing upwards for healthy cells.

In addition to extensive laboratory testing under 1 g conditions, our system has been successfully used in a parabolic flight campaign in Bordeaux (F) under the auspices of the European Space Agency (ESA) and in the Large Diameter Centrifuge (LDC) at the European Space Research and Technology Center (ESTEC) at Noordwijk (NL).

Principle of the ATOVC

Previously described electrophysiology techniques such as the TOVC[23] and the loose macropatch voltage clamp[21, 22] do not involve physical disruption of the membrane and therefore allow non-invasive electrophysiological measurements of membrane protein activity. For the TOVC, the oocyte is positioned in an orifice separating two fluid-filled compartments resembling an Ussing chamber and the electrical potential between the compartments is controlled to measure the transoocyte current. This arrangement has been used for transoocyte noise and impedance measurements.[23] In the loose macropatch,[21, 22] the extracellular potential is operator-defined and current is measured from a small membrane patch by means of a glass pipette that lightly touches the cell membrane. For both methods, some of the current measured results from leakage because the membrane is not perfectly sealed to the orifice or patch pipette, respectively. Importantly, the transmembrane potential is poorly defined because the intracellular potential is unknown and in the case of large currents, errors in membrane voltage control may occur. One solution to this problem was recently described by Dahan et al.,[14] in which a defined area of the oocyte membrane was permeabilised using an ionophore to allow a low resistance access to the cytosol.

As in the Dahan approach, we have used a conical structure with a small hole which separates the two fluid filled compartments. With the oocyte in place, this effectively divides the oocyte membrane surface into a lower "patched" region that is exposed to a microfluidic perfusion channel, and an upper "body" region that is exposed to the upper compartment. The surface area of the patch membrane is much smaller than the surface area of the entire oocyte (Fig. S2, S3) and in this context, the arrangement can be considered a variation of the loose macropatch.[21, 22] By defining the electrical potentials in the two compartments, our system offers the flexibility of allowing transoocyte impedance measurements as for the TOVC[23]; loose macropatch measurements[21, 22] and, by permeabilising the body membrane, we can gain electrical access to the cytosol.[14] Due to the uneven surface topology of the oocyte membrane and associated vitelline layer,[26] it is impossible to fully prevent ohmic leakage currents passing around the cell between the two compartments. However, these leak currents will remain constant, assuming the oocyte is stabilised. Moreover, they can be eliminated when control and test recordings are subtracted from one another.

Materials and methods

Fabrication of the core microfluidic module

The design and realisation of the microfluidic module is

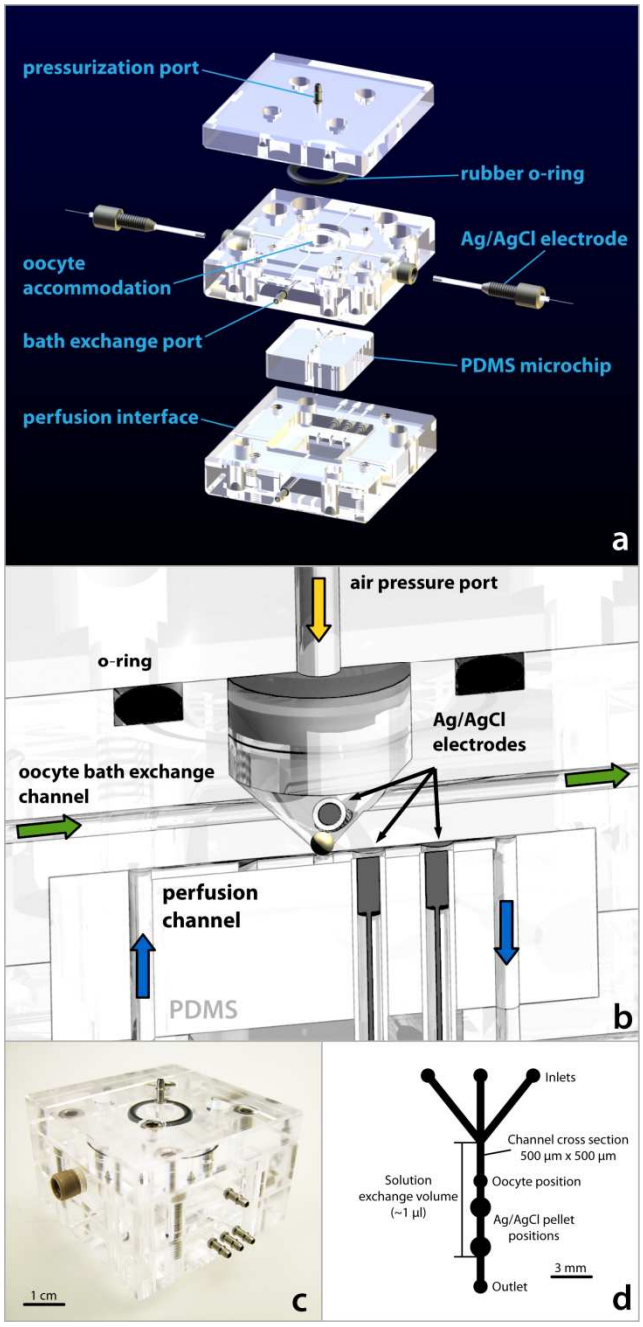

Fig. 1 (a) Exploded view of rendered 3D CAD data used for the fabrication of the PMMA parts. The bottom electrodes are inserted into the PDMS microchip using 1/16 inch PFA tubing as a sleeve (tubing not shown for clarity). (b) Cross-section view of rendered 3D CAD schematic of the assembled microfluidic module. (c) Photograph of the microfluidic module. (d) Design of the microfluidic channels in PDMS. The solution exchange volume is given approximately by the length of the main channel times its cross sectional area (in our case approx. 1 µl). The exact volume is smaller due to the protrusion of the pellet electrodes and part of the oocyte patch into the channel.

shown in Fig. 1. The perfusion microchip was made of PDMS (Sylgard, Dow Corning) by moulding from a structured silicon wafer.[27] The wafer was made from a high-viscosity positive resist (SU-8 2100, Microchem) employing standard lithography technology. Using a slow spinning step (500 RPM for 30 s), a final structure height of approximately 500 µm was obtained. This channel height was chosen to minimise the susceptibility to channel blockage should the oocyte become damaged and pass through the hole and to facilitate the integration of the Ag/AgCl electrodes. A precisely machined polytetrafluoroethylene (PTFE) frame was aligned with the master structures to obtain a PDMS microchip with exact dimensions on all axes (24 x 24 x 8mm^3) and a centred microfluidic structure. Well-defined curing conditions were used to keep the shrinkage of PDMS constant.[28] A ratio of 1:8 of curing agent to prepolymer was used for easier removal of the cured PDMS from its mould and for higher dimensional stability. Curing was done in an oven at 100°C for 1 hour. After removal of the PDMS microchip from its mould, 1 mm wide holes were punched at predefined positions using a biopsy puncher. These access holes were necessary for interfacing the fluid pathways and the sintered Ag/AgCl electrodes (Ag/AgCl 1 mm pellets, Warner Instruments, CT). The perfusion microchip was finally integrated with 3 CNC-machined polymethylmethacrylate (PMMA) parts that serve multiple functions such as interfacing, sealing and oocyte accommodation (Fig. 1a).

An important feature of the assembly is the clamping of the PDMS microchip between the PMMA parts. The thickness of the microchip is slightly larger than the cavity of the PMMA parts, resulting in compression of the microchip and perfect sealing of the microfluidic pathways. Moreover, as a result of the PDMS moulding process, the oocyte patch hole in the PMMA is automatically aligned with the perfusion channel when the device is assembled.

In the present system we opted for a 300 µm diameter patch hole, which results in a sphere to patch surface ratio of 43 (Fig. S3a), giving a good compromise between electrical access to the cytosol, signal-to-noise ratio and mechanical stability.

Realisation of the peripheral fluidic and air pressure system

The scheme of the fully closed peripheral system is depicted in Fig. 2. To provide the pressure source we used a small air bottle (Sure/Pac 275 ml, Sigma-Aldrich). To control the pressure on the fluids, we used an electronic pressure regulator with feedback control (T3110, 1000 mbar, Marsh-Bellofram). The output pressure of the regulator pressurised glass vials filled with the perfusion fluids. Switching between the fluids was achieved by using solenoid valves (LFVA1220110H, Lee Co.). Teflon capillary tubes (0.25 mm inner diameter, 30 cm length) between the solution vials and the solenoid valves ensured a well-defined steady-state flow rate through the microfluidic module. To reduce the water hammer effect resulting from the switching action of the valves, air pocket elements between the valves and the microfluidic device were introduced. The outlet of the microfluidic device was connected to an expandable polypropylene reservoir[29] acting as a sealed waste container. For the pressurization of the oocyte a second pressure regulator was used (T3110, 68 mbar, Marsh-Bellofram). To avoid large pressure transients and fluctuations a compensation volume between the regulator and the microfluidic device was introduced.

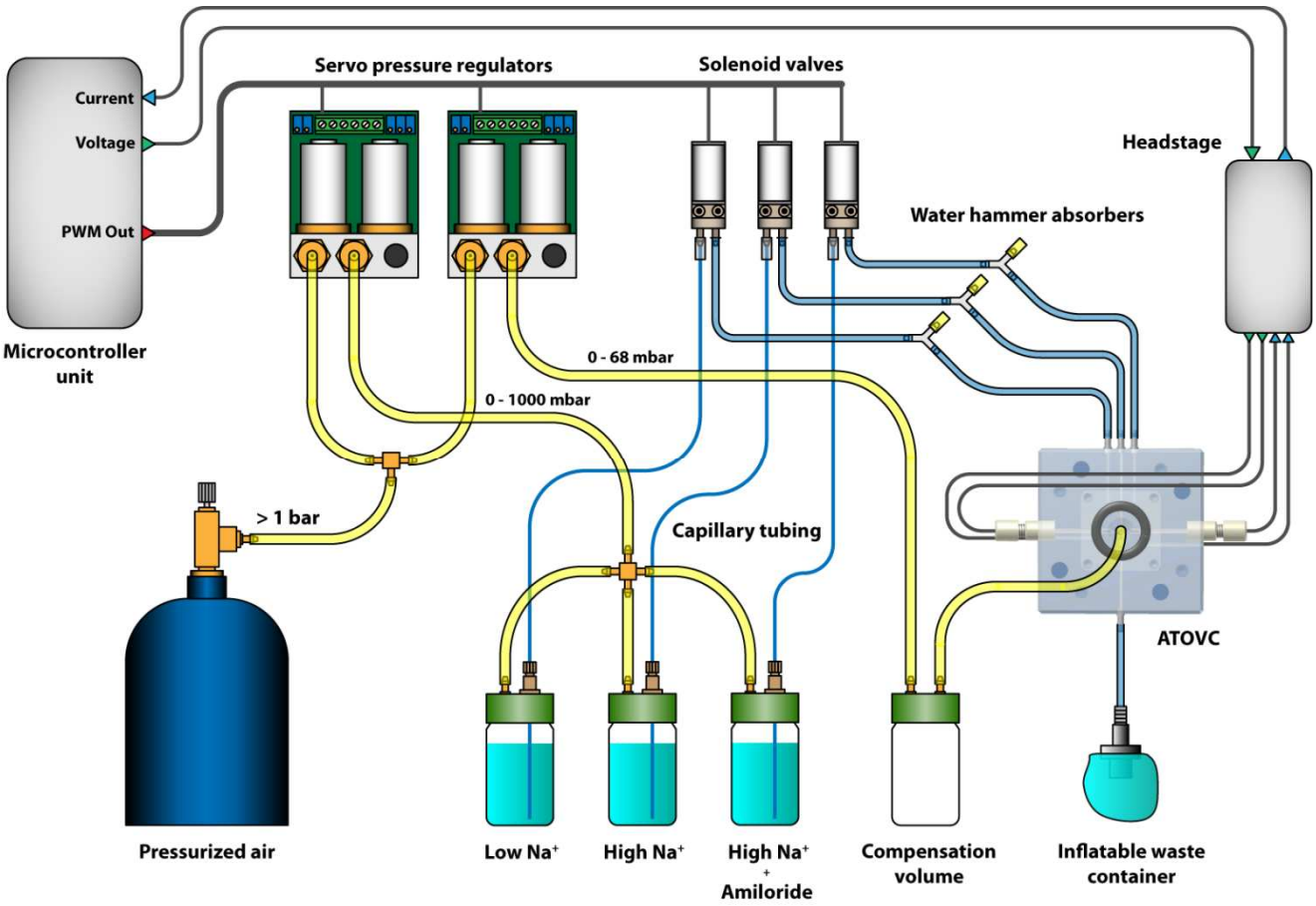

Fig. 2 Schematic of the peripheral system. Yellow denotes air, blue denotes liquid and grey denotes an electrical connection.

Reagents and solutions

Modified Barth's solution for storing oocytes contained (in mM): 88 NaCl, 1 KCl, 0.41 $CaCl_2$, 0.82 $MgSO_4$, 2.5 $NaHCO_3$, 2 $Ca(NO_3)_2$, 7.5 HEPES. The solution was adjusted to pH 7.5 with Tris and supplemented with 5 mg/l doxycycline and 5 mg/l gentamicine. For storage of oocytes after the injection, a low Na^+ Barth's solution was used with the Na^+ concentration reduced to 10 mM and replaced with 78 mM methyl-d-glucamine (NMDG). Standard extracellular solution (100Na) contained (in mM): 100 NaCl, 2 KCl, 1.8 $CaCl_2$, 10 HEPES, pH 7.4 adjusted with TRIS. The 10 mM Na^+ test solution (10Na) had the same composition as 100Na except that 90 mM of the NaCl was replaced with choline chloride. For test solutions containing amiloride, this was added from 100 mM stock (in DMSO) immediately prior to priming the solution reservoirs (see below) to give a final concentration of 10 μM. All standard reagents were obtained from either Sigma-Aldrich or Fluka.

Oocyte preparation

Female *X. laevis* frogs were purchased from *Xenopus* Express (France) or African *Xenopus* Facility (R. South Africa). Portions of ovaries were surgically removed from frogs anesthetized in MS222 (tricaine methanesulphonate) and cut in small pieces. Oocytes were treated for 45 min with collagenase (crude type 1A) 1 mg/ml in 100Na solution (without Ca^{2+}) in presence of 0.1 mg/ml trypsin inhibitor type III-O. Healthy stage V-VI oocytes were selected, maintained in modified Barth's solution at 16 °C and injected with 5 ng total of cRNA of the α,β,γ sub-units of the *Xenopus* isoform of ENaC according to previously described procedures in our laboratory.[30] After injection, the oocytes were incubated for 3 days at 16 °C in the low Na^+ Barth's solution (10 mM) to maintain a low intracellular Na^+ concentration and ensure cell survival. Non-injected oocytes of the same batch were used as a negative control as the amiloride-sensitive inhibition of endogenous mechanically sensitive channels is only detected under tight seal patch conditions and the microvilli and invaginations present in the healthy stage VI oocyte membrane are thought to buffer direct mechanical activation of these channels in the intact oocyte. [31, 32]

Voltage clamp hardware and system controller

The general arrangement of the voltage clamping hardware configuration is detailed in the ESI (Fig. S1). It was designed to be easily adapted to perform different electrophysiological measurements such as transimpedance and loose macropatch voltage clamping. For the experiments described in the present study, aimed at voltage clamping the patch membrane itself, the electrical potential in the compartment facing the oocyte patch (microfluidics channel) was defined as signal ground by means of a virtual ground amplifier connected to the two electrodes in the microfluidics channel. The electrical

potential in the upper compartment was defined by the input command potential using a conventional two electrode voltage clamp (TEVC) arrangement connected to the two upper compartment electrodes. The analogue command potential, defined according to the proprietary control software, was generated by a 16 bit DAC in the microcontroller unit. Two analogue signals were measured: the potential of the upper compartment and net current passing between the two compartments. They were acquired by 16 bit ADC's in the microcontroller unit with timing and sampling rates defined by the proprietary software user interface. Data were written automatically to a removable solid-state memory device. The pressure controllers and fluid solenoid valves were driven from the microcontroller unit by pulse width modulation and TTL signals, respectively. The microcontroller unit was a fully customised design (Interstate University for Technology Buchs (NTB), Switzerland) based on the MPC555 microcontroller with a number of connected peripherals. The unit could be connected to a computer for direct human control or operated fully automatically with data continuously written to removable media via a USB interface.

Results

System evaluation under standard laboratory conditions

We first optimised the entire system in the laboratory environment to verify its robustness and ease of operation. The best conditions for cell immobilisation were evaluated. To ensure the cell remained correctly and stably positioned on the patch hole, we applied a constant and well-defined air pressure to the upper compartment. This pressure served two purposes: (i) it increased the leak resistance between the two compartments around the oocyte by counteracting forces acting on the oocyte resulting from the flow inside the perfusion channel - if the air pressure in the bath is high compared to the pressure resulting from the perfusion flow, the leak resistance will become independent of the flow rate inside the perfusion channel; (ii) when in operation it served to ensure that any effects of gravitational forces on the leak resistance were negligible and therefore allowed the system to operate under microgravity conditions. Tests for determining the influence of variations in the pressure differentials on the leak resistance were performed to demonstrate its low susceptibility to changing environmental conditions (Fig. S6).

To demonstrate the viability of the system for monitoring the membrane conductance change of the patch under voltage clamp conditions, we used oocytes that overexpressed a channel with known properties, namely the epithelial sodium channel (ENaC). The large macroscopic conductance associated with ENaC expression meant that the conductance of the cell membrane exposed to the upper compartment established a low resistance electrical access to the cytosol and the cytosolic side of the patch.[‡] Moreover, as ENaC can be reversibly blocked by application of the inhibitor amiloride, the leak current between the two compartments could be eliminated by subtraction of recordings made in the presence of amiloride from control recordings. For these experiments, the perfusion system was filled with the 100Na,

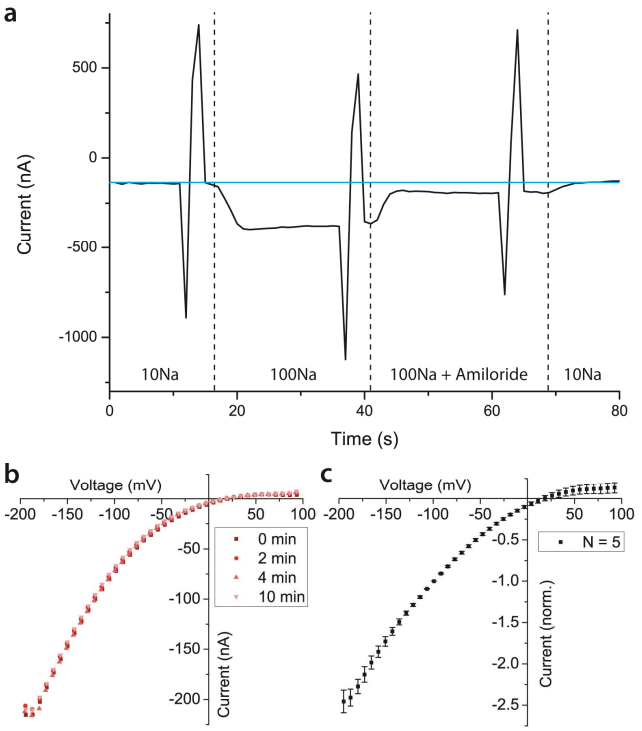

Fig. 3 (a) Real-time current measurement on an ENaC expressing oocyte. The transoocyte voltage was kept constant at -50 mV except immediately before switching solutions where voltage sweeps where applied as indicated. The blue line represents the initial current demonstrating the steady-state stability before and after the solution switching procedure. The flow rate was kept constant at 1 µl/s. (b) Four I-V curves from one selected oocyte measured consecutively at the times indicated. (c) I-V curve representing the average of 5 oocytes and normalized to the current at -100 mV. The mean reversal potential is approx. +20 mV. For the data in plots b and c a voltage ramp from -200 mV to +100 mV with a period of 20 s was applied.

100Na + amiloride and 10Na solutions, and the oocyte was placed in the chamber together with approximately 200 µl of 10Na solution. The amiloride concentration (10 µM) was used to ensure the complete inhibition of all ENaCs exposed to the microperfusion channel.[33] The top PMMA plate was positioned and fixed with screws and the oocyte compartment was pressurised at 20 mbar. Various leak evaluation tests had shown that this value was the best compromise between maximising the leak resistance (typically in the range of 150 to 200 kΩ for 10Na) and minimising stress to the oocyte membrane. We found that increasing the pressure beyond 20 mbar did not yield a substantial increase in leak resistance, most probably because the area of the contact between the oocyte and funnel remained unchanged and the oocyte would simply be pushed through the hole further. Furthermore, oocytes pressurized at 50 mbar and beyond tended to burst after a few minutes.

After top pressurization, the perfusion system was started and the oocyte constantly perfused with 10Na solution to replicate the standard incubation conditions and avoid loading the cells with sodium. It was found that the oocyte typically required 3 to 5 minutes to reach a stable condition after starting pressurization. The perfusion sequence was then initiated (Fig. 3a), which consisted of switching from 10Na

solution to perfusion with 100Na solution for 10-20 s followed by 100Na solution containing 10 µM amiloride for 10-20 s. This was followed by a washout in 10Na solution to return to the initial conditions. The individual steps of the perfusion procedure as well as the measurement parameters were configured by the software. Two electrophysiological characterisations were performed using the system: time-dependent current measurements at a constant holding potential and current-voltage (I-V) characterizations using a voltage ramp or voltage step sequence.

Fig. 3a shows a representative steady-state recording at a transoocyte potential of -50 mV (upper compartment relative to lower compartment) for an ENaC overexpressing oocyte subjected to the perfusion sequence indicated. Assuming a solution exchange volume of approximately 1 µl, the solution exchange time is around 1 s for the flow rate we used (1 µl/s, Fig. 3a), giving reasonable response time of the microfluidic exchange. The rapid response to the application of amiloride within a few seconds for the ATOVC confirms the good performance of this system. The I-V relation of the amiloride-sensitive current (Fig. 3b) for repeated applications and wash-out on the same oocyte at the time intervals indicated shows that the system responded reproducibly with little change in the currents between successive measurements. For this cell, the reversal potential remained constant and indicated that the internal [Na^+] did not change significantly between successive measurements. Moreover, comparison of I-V traces agreed well with the TEVC recording (Fig. S5b).

The curvilinear nature of the I-V reflects the typical amiloride-sensitive macroscopic current carried by ENaC as previously reported.[34] This characteristic shape was found for oocytes overexpressing different levels of ENaC. Fig. 3c shows the I-V traces obtained from 5 different oocytes with amiloride-sensitive currents varying from -28 nA to -80 nA (at -50 mV). The data were normalized to the current at -100 mV and superimposed to show that the voltage dependence was unchanged, independent of expression level. The reversal potential of (+20 ± 10) mV is lower than predicted (+59 mV) from the assumed 10:1 Na concentration gradient across the patch membrane. As this did not change significantly with expression level it is unlikely that it resulted from inadequate voltage control of the patch membrane, but rather suggests that the internal [Na^+] was higher than assumed.

Finally, we tested the system on two different laboratory shakers providing either horizontal or wave-like movements (see ESI, movie 1 and 2). The output signals were not affected by the movement, which confirmed the high stability and robustness of the system.

Measurements under hypergravity

To study if extended periods of hypergravity affected the macroscopic conductance of ENaC overexpressing oocytes, we conducted tests on a Large Diameter Centrifuge (LDC) provided at the European Space Research and Technology Center (ESTEC) at Noordwijk (NL). The entire system was mounted in a centrifugation chamber and exposed to 1.8 g for about 20 minutes. After an initial time of about 2 minutes to allow cell settlement on the hole, the complete experimental protocol, including solution exchange and current recording, was remotely triggered at defined time intervals varying from 90 seconds to 5 minutes.

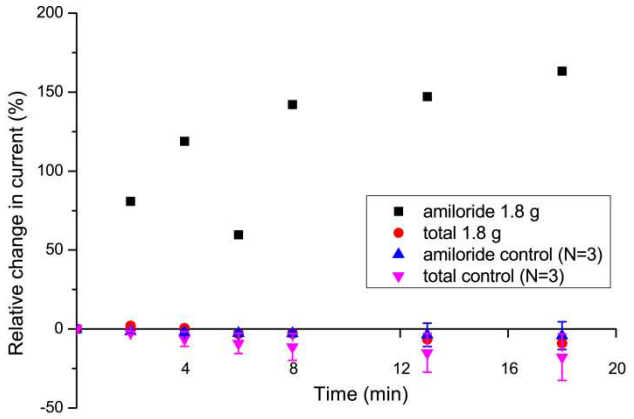

Fig. 4 Results of ATOVC measurements from two representative ENaC overexpressing oocytes at 1 g and 1.8 g. Hypergravity was achieved using a Large Diameter Centrifuge. After a short stabilisation time of about 2 min, the relative changes of the total current at 100Na and the relative changes of the amiloride-sensitive current over a time course of 18 minutes were recorded. The transoocyte potential was held constant at -100 mV.

In Fig. 4 the relative changes of total and amiloride-sensitive currents are shown for an oocyte overexpressing ENaC that was exposed to hypergravity and compared to the results obtained for another oocyte exposed to the same experimental protocol at 1 g but with an immobilisation pressure of 20.5 mbar to account for the increased hydrostatic pressure under hypergravity. Analysis of the data revealed that under these conditions, the amiloride-sensitive current increased to 150 % of the initial value, whereas the total current decreased slightly (Fig. 4). In contrast, for the oocyte on the ground (1 g), we observed an insignificant change in amiloride-sensitive current, and a slight decrease in the total current (leak plus oocyte current), which was comparable to the 1.8 g experiment. Taken together, these findings indicated that the increase in amiloride-sensitive current under hypergravity could not be attributed to either changes in patch size (i.e. an increase in the number of channels exposed to amiloride) or leak conductance. These findings strongly suggested that exposure to hypergravity appeared to influence the sodium conductance mediated by ENaC.

Measurements during a parabolic flight

Two ATOVC systems were fixed on a stable baseplate, which was mounted within a metal enclosure in the aeroplane used for parabolic manoeuvres (Fig. S7). It was mandatory that no access to the enclosure was possible during each set of parabolic manoeuvres and therefore the entire measurement protocol was fully automated, with controls and real-time monitoring via a customised touch-screen interface. Each manoeuvre comprised two hyper-g (ca. 1.8 g) phases that bracketed the nominal micro-g phase. A typical flight involved a total of 31 such manoeuvres. Before the flights, oocytes were freshly prepared and stored on site. They were

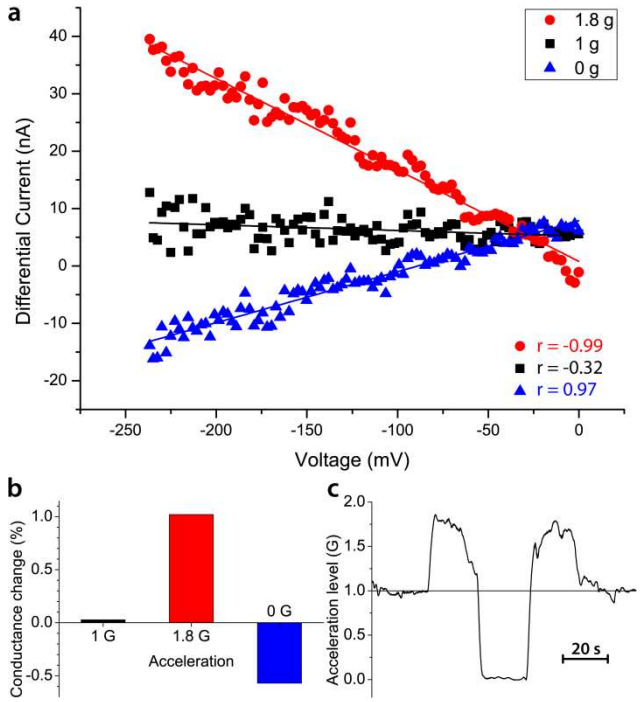

Fig. 5 (a) Differential current of an ENaC overexpressing oocyte recorded during a parabolic flight manoeuvre. The I-V curve for each acceleration level was subtracted from that recorded prior to the manoeuvre. The 1 g trace was obtained by subtracting the I-V curves taken directly before and after the manoeuvre. Linear regression was applied to the datasets yielding the change in conductance for the slope (Pearson's coefficients are shown on the bottom right of the graph) (b) Plot of the relative differential conductance resulting from the I-V data shown in a. (c) Readout of the on-board accelerometer during a parabolic manoeuvre. The sense of the acceleration vector was from the upper compartment of the core module to the microperfusion channel.

introduced into the core module prior to each set of 5 parabolas.

Fig. 5a shows first data obtained from an ENaC overexpressing oocyte that was exposed to several hyper- and microgravity phases. Here we compared for a single oocyte the change in total current (leak plus transoocyte current) of each phase with respect to the normal gravity condition before the manoeuvre. By subtracting the I-V data obtained during each phase from the I-V curve before the manoeuvre, the difference in transoocyte conductance is obtained. The resulting I-V curves can be fitted with a linear function from which we can estimate the transoocyte conductance. In our case, changes in transoocyte conductance were seen during hyper- and zero gravity conditions (Fig. 5b, c). Comparison with the conductance before and after the parabolic manoeuvre showed no significant change, which suggested that the oocyte reverted to initial conditions after the manoeuvre. The origin of these phenomena has yet to be elucidated, and it appears unlikely that they result from systematic errors due to alternating changes in leak resistance during micro- and hypergravity, which we found to be minimal. In particular, the contribution of the gravitational force to the total force acting on the entire oocyte can easily be estimated. For a typical oocyte diameter of 1 mm and a stabilising air pressure of 20 mbar, the gravitational force is approximately 1000-fold smaller than the force applied to the oocyte via positive pressure.[§] The contribution of the change in hydrostatic pressure (approx. 0.5 mbar per g) to the leak conductance is less than 2 nA at -50 mV transoocyte voltage (Fig. S6b). Therefore, we believe that the changes can indeed be assigned to the response of the oocyte to alteration in the gravity level. However, further studies are required to confirm the results and reveal the underlying mechanisms.

Conclusions

We describe a system for performing non-invasive electrophysiological measurements on *Xenopus laevis* oocytes under varying gravity levels. Benchmark experiments conducted in the laboratory demonstrate that our system is able to faithfully reproduce the results typically obtained by the TEVC method. Furthermore, due to the high stability of the leak current, we were able to measure changes in current with nanoampere resolution. Initial results on ENaC overexpressing oocytes exposed to micro- and hypergravity have been presented that suggest ENaC activity is indeed sensitive to gravitational forces. Future analysis of other ion channel classes under micro- or hypergravity will certainly provide additional biologically relevant insights, into which physiological pathways are affected by gravitational change.

The key advantages of this system, in accordance with our stringent design criteria, are: (i) the very short time needed for setup and measurement, (ii) capability of fully automatic operation (after mounting the oocyte) and (iii) high reliability. Although the system was developed specifically for electrophysiological studies under varying gravity conditions, due to its operational simplicity it could also be conveniently used for electrophysiological investigations in ground-based laboratories.

Acknowledgements

We acknowledge the fruitful initial discussions with Prof. M.A.M. Gijs, Dr. T. Lehnert (EPFL, CH) and Dr. V. Bize (University of Lausanne, CH) with regard to the adaptation of the ATOVC design. We acknowledge support from Beat Huber and Christoph Bärtschi for the fabrication of the mechanical parts and Interstate University for Technology Buchs (NTB) for the development and fabrication of the voltage clamp & system controller. We thank the European Space Agency (ESA) for the opportunity to participate in the parabolic flight campaigns. Furthermore, we thank Novespace for the organisation of the parabolic flights as well as for their assistance. In addition we thank ESA for the opportunity to participate in their "Spin your thesis" initiative. We gratefully acknowledge financial contribution from Novartis (International Doctoral Fellowship 2009) to D.S. and the European Research Council (ERC Starting Grant, nμ-LIPIDS, No. 203428) to P.S.D. and the Innovation Triangle Initiative (ITI) of ESA for project funding to M.E. We thank Eva Hänsenberger and Monica Patti (Institute of Physiology, UZH) for expert preparation of oocytes and Michel Möckli for technical assistance with the electronic hardware.

References

[a] *Department of Chemistry and Applied Biosciences, ETH Zurich, CH-8093 Zurich, Switzerland. E-mail: dittrich@org.chem.ethz.ch*
[b] *Institute of Physiology and ZIHP (Center for Integrated Human Physiology), University of Zurich, CH-8057 Zurich, Switzerland. E-mail: iforster@access.uzh.ch*
[c] *Space Biology Group, ETH Zurich, CH-8005 Zurich, Switzerland. E-mail: marcel.egli@spacebiol.ethz.ch*

† Electronic Supplementary Information (ESI) available: Voltage clamp configuration, Calculation of the patch surface area, Leak conductance stability tests, Numerical impedance analysis of the ATOVC, TEVC reference measurements, Photograph of the ATOVC setup for parabolic flights, and two movies.

1 A. Franco-Obregon, H. W. Wang and D. E. Clapham, *Biophys J*, 2000, **79**, 202-214.
2 F. M. Ashcroft, 2000.
3 M. Fronius and W. G. Clauss, *Pflug Arch Eur J Phys*, 2008, **455**, 775-785.
4 A. G. Petrov, B. A. Miller, K. Hristova and P. N. Usherwood, *Eur Biophys J*, 1993, **22**, 289-300.
5 R. Hemmersbach, M. Krause, R. Bräucker and K. Ivanova, *Adv Space Res*, 2005, **35**, 296-299.
6 M. Toyota, T. Furuichi, H. Tatsumi and M. Sokabe, *Plant Physiol*, 2008, **146**, 505-514.
7 E. Blaber, H. Marcal and B. P. Burns, *Astrobiology*, 2010, **10**, 463-473.
8 P. E. Di Prampero, M. V. Narici and P. A. Tesch, eds., *A world without gravity*, European Space Agency, 2001.
9 E. L. Kordyum, *Cell Biol Int*, 2003, **27**, 219-221.
10 J. B. Lansman and A. Franco-Obregon, *Clin Exp Pharmacol Physiol*, 2006, **33**, 649-656.
11 K. G. Klemic, J. F. Klemic, M. A. Reed and F. J. Sigworth, *Biosens Bioelectron*, 2002, **17**, 597-604.
12 K. G. Klemic, J. F. Klemic and F. J. Sigworth, *Pflug Arch Eur J Phy*, 2005, **449**, 564-572.
13 N. Fertig, R. H. Blick and J. C. Behrends, *Biophys J*, 2002, **82**, 3056-3062.
14 E. Dahan, V. Bize, T. Lehnert, J. D. Horisberger and M. A. M. Gijs, *Lab Chip*, 2008, **8**, 1809-1818.
15 S. Dharia, H. E. Ayliffe and R. D. Rabbitt, *Lab Chip*, 2009, **9**, 3370-3377.
16 A. Y. Lau, P. J. Hung, A. R. Wu and L. P. Lee, *Lab Chip*, 2006, **6**, 1510-1515.
17 T. Y. Tu, *Proc. of the μTAS conference*, Groningen 2010, 929-931.
18 M. Estacion, J. S. Choi, E. M. Eastman, Z. Lin, Y. Li, L. Tyrrell, Y. Yang, S. D. Dib-Hajj and S. G. Waxman, *J Physiol*, 2010, **588**, 1915-1927.
19 T. Fukuba, T. Naganuma and T. Fujii, *Proc. Int. Symp. Underwater Technology*, 2002, 101-105.
20 P. A. Willis, F. Greer, M. C. Lee, J. A. Smith, V. E. White, F. J. Grunthaner, J. J. Sprague and J. P. Rolland, *Lab Chip*, 2008, **8**, 1024-1026.
21 W. M. Roberts and W. Almers, *Methods Enzymol*, 1992, **207**, 155-176.
22 A. Strickholm, *J Gen Physiol*, 1961, **44**, 1073-1088.
23 D. Cucu, J. Simaels, D. Jans and W. Van Driessche, *Pflug Arch Eur J Phys*, 2004, **447**, 934-942.
24 M. Althaus, R. Bogdan, W. G. Clauss and M. Fronius, *Faseb J*, 2007, **21**, 2389-2399.
25 A. Simon, F. Shenton, I. Hunter, R. W. Banks and G. S. Bewick, *J Physiol*, 2010, **588**, 171-185.
26 H. G. Callan and S. G. Tomlin, *P Roy Soc Lond B Bio*, 1950, **137**, 367-378.
27 D. C. Duffy, J. C. McDonald, O. J. A. Schueller and G. M. Whitesides, *Anal Chem*, 1998, **70**, 4974-4984.
28 S. W. Lee and S. S. Lee, *Microsyst Technol*, 2007, **14**, 205-208.
29 I. Walther, B. H. van der Schoot, S. Jeanneret, P. Arquint, N. F. de Rooij, V. Gass, B. Bechler, G. Lorenzi and A. Cogoli, *J Biotechnol*, 1994, **38**, 21-32.
30 P. Fakitsas, G. Adam, D. Daidie, M. X. van Bemmelen, F. Fouladkou, A. Patrignani, U. Wagner, R. Warth, S. M. Camargo, O. Staub and F. Verrey, *J Am Soc Nephrol*, 2007, **18**, 1084-1092.
31 O. P. Hamill and B. Martinac, *Physiol Rev*, 2001, **81**, 685-740.
32 J. W. Lane, D. W. McBride, Jr. and O. P. Hamill, *Br J Pharmacol*, 1993, **108**, 116-119.
33 H. Garty and L. G. Palmer, *Physiol Rev*, 1997, **77**, 359-396.
34 V. Bize and J. D. Horisberger, *Am J Physiol Renal Physiol*, 2007, **293**, F1137-1146.

‡ Permeabilisation of the body membrane could also be achieved using ionophores as demonstrated by Dahan et al.[14] In the present design, a perfusion pathway was already incorporated (Fig. 1b) to allow changes in upper compartment composition and this could be adapted for the permeabilisation procedure

§ For this calculation the values for the force resulting from the air pressure and the oocyte weight are assumed to be $4\pi R^2 p$ and $4/3\pi R^3 \rho g$, respectively. For ρ we chose a value of 1.2 g/cm^3 due to the oocyte's slightly higher mass density compared to water.

Supplementary information

Description of the ATOVC

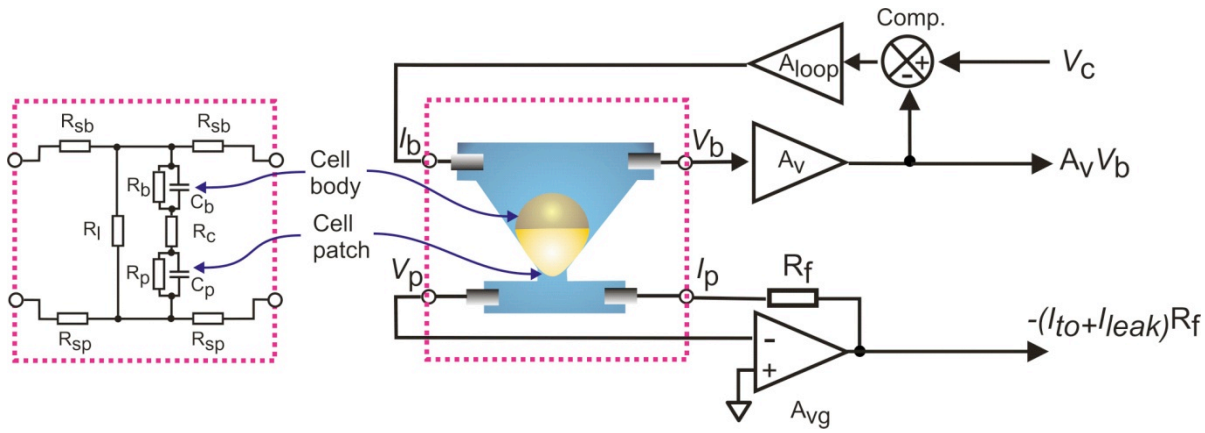

Fig. S1 Simplified schematic of the ATOVC (not drawn to scale) as used for the experiments described, in which the body membrane exposed to the upper compartment fluid is permeabilized to gain electrical access to the cytosol and thereby allow voltage clamping of the patch exposed to the lower compartment (microfluidic channel). Two electrodes make contact with solution in the upper compartment (I_b, V_b) and lower compartment (I_p, V_p) respectively. The equivalent circuit of the boxed region, representing the oocyte positioned in the core module, is also depicted. This is an AC equivalent model used in simulations (see below) and omits the membrane potential. R_{sb} and R_{sp} represent the equivalent resistances of the electrodes and fluid access to the body (upper) and patch (lower) membranes, R_l is the leak resistance, R_b and C_b are the lumped resistance and capacitance of the cell body, Rc is the lumped cytosolic resistance and R_P and C_P are the membrane patch resistance and capacitance, respectively. The voltage clamp electronics comprises two components that connect to the lower and upper compartments, respectively: (i) a virtual ground amplifier (A_{vg}) defines the potential in the lower compartment (approximating the potential at the external surface of the patch) to 0 V and acts as a transimpedance stage that outputs a voltage proportional to the total current (leak (I_{leak}) and transoocyte (I_{to})); (ii) a feedback amplifier arrangement, comprising amplifier A_v, a comparator and loop gain amplifier (A_{loop}) senses the electrical potential in the upper compartment and compares a scaled version of this (A_v V_b) to the external command voltage input (V_c). The feedback amplifier (A_{loop}) drives current (I_{leak} + I_{to}) to maintain the transoocyte potential at the desired value.

The arrangement shown in Fig S1 permits voltage clamping of the patch membrane by controlling the cytosolic potential and assumes adequate electrical access to the cytosol from the upper compartment has been established. The same arrangement could be used for transimpedance measurements. Furthermore, by rearranging the connections to the core module so that the potential in the lower compartment is externally defined, and the upper compartment is held at 0 V, a loose macropatch configuration would be created.

Patch surface area considerations

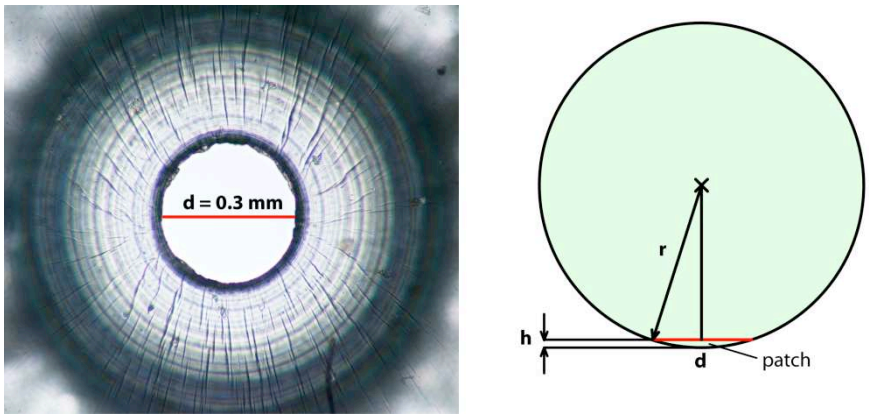

Fig. S2 Left: Micrograph showing the oocyte immobilization site from above. The patch hole diameter is 0.3 mm. Right: Idealised cross-section of the oocyte showing geometrical parameters.

The patch opening diameter was chosen on the basis of maintaining cell stability, considerations of the electrical properties of the cell and having rapid superfusion of the exposed area. Too large an opening would result in poor electrical access to the cytosol whereas too small an opening would compromise the signal-to-noise ratio for the patch current.
The surface area (S) of a sphere with radius r is given by: $S = 4 \pi r^2$.
The patch area (curved surface area of the cap) is calculated using the following equations: $S_P = 2 \pi r h$ with $h = r - \sqrt{(r^2 - a^2)}$.
where, h is the height of the patch and a the patch radius. For a sphere with r=0.5 mm (typical for *Xenopus laevis* oocytes) and a =0.15 mm (Fig. S2) the surface area ratio is:

$$\frac{S}{S_P} \approx 43$$

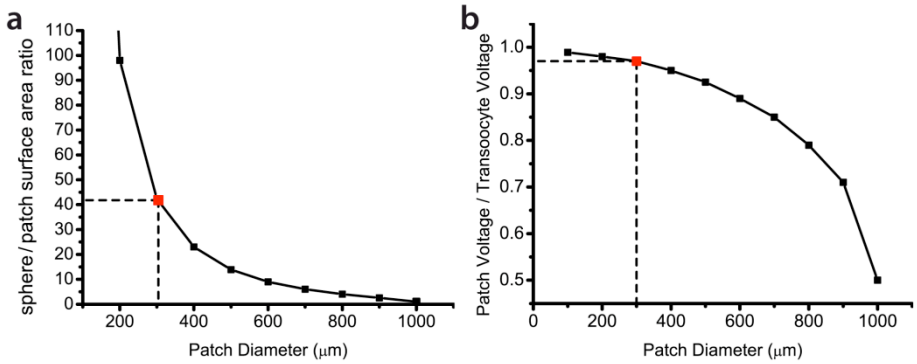

Fig. S3 The dependence of the surface ratio (a) and voltage ratio (b) plotted as function of the patch hole diameter. The values were obtained by simulation (Fig. S4) for a typical oocyte diameter of 1 mm and an AC clamp voltage at 10 Hz. Actual values chosen for our design are indicated (dashed lines/red symbols).

The relationship between the impedance ratio of the two membrane parts and their respective surface areas can be expressed using the following equation:

$$\frac{R_B}{R_P} = \frac{C_P}{C_B} = \frac{4\pi r^2}{S_P} - 1$$

where r: radius of the oocyte and S_P: patch area. Here we take the apparent geometrical areas and ignore the increased surface area of the oocyte due to the microvilli and invaginations. This would simply scale the calculated areas equally.

Assuming homogeneous distribution of membrane conductance the membrane impedances of the two regions will differ, according to the ratio of the membrane areas of each region. Consequently, changes in the transoocyte current will mainly result from changes in the impedance of the patch membrane due to its much higher impedance compared to the impedance of the body membrane.

Thus, even though the oocyte is effectively voltage clamped across two membranes, the largest fraction of applied AC voltage falls across the patched membrane, i.e. by having a large ratio between the non-patched area and the patched area, a voltage clamp from the cytosol across a single membrane is approximated (Fig. S3b). In practice, the measured values will deviate somewhat from the calculated values due to the deformation of the immobilized oocyte. Nevertheless, this relation is useful for comparing membrane currents of the ATOVC with membrane currents measured with a conventional instrument (TEVC). Moreover, to simplify the analysis, this model ignores the effect of inhomogeneities of membrane access resistance close to the patch hole.

AC impedance analysis of the ATOVC

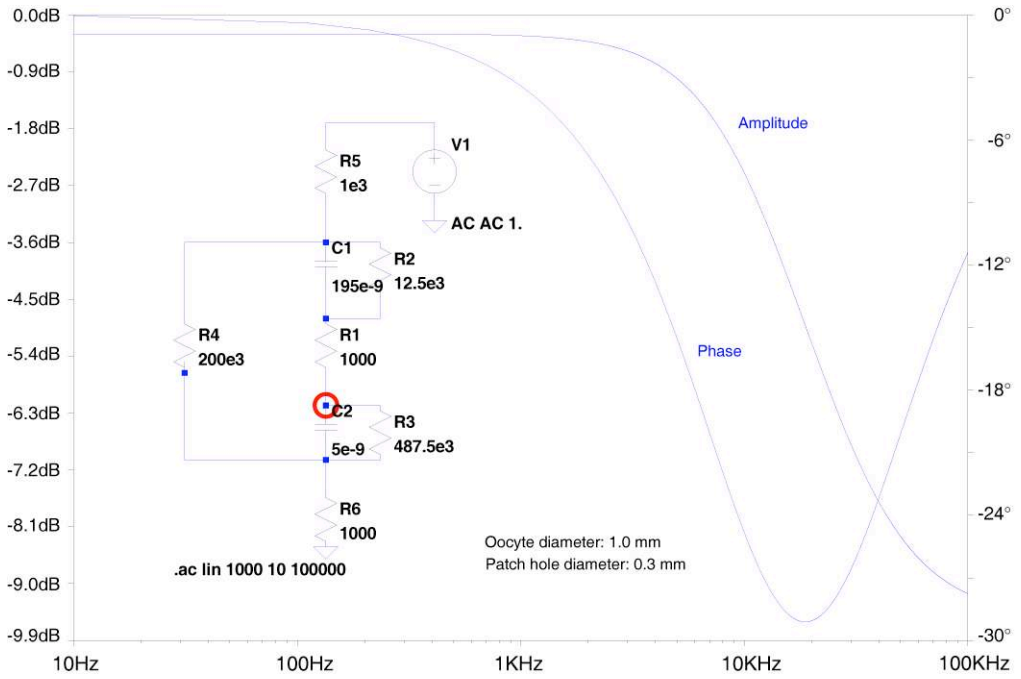

Fig. S4 Bode plot of the equivalent circuit of the ATOVC (made using LT SPICE IV (Linear Technologies)). The absolute values for the resistances and capacitances are rough estimates. The DC resistance of the entire circuit is typically around 150 kΩ.

A SPICE AC analysis using estimated values for the ATOVC reveals that the patch impedance is reasonably constant up to frequencies around 1 kHz (Fig. S4).

TEVC reference measurements

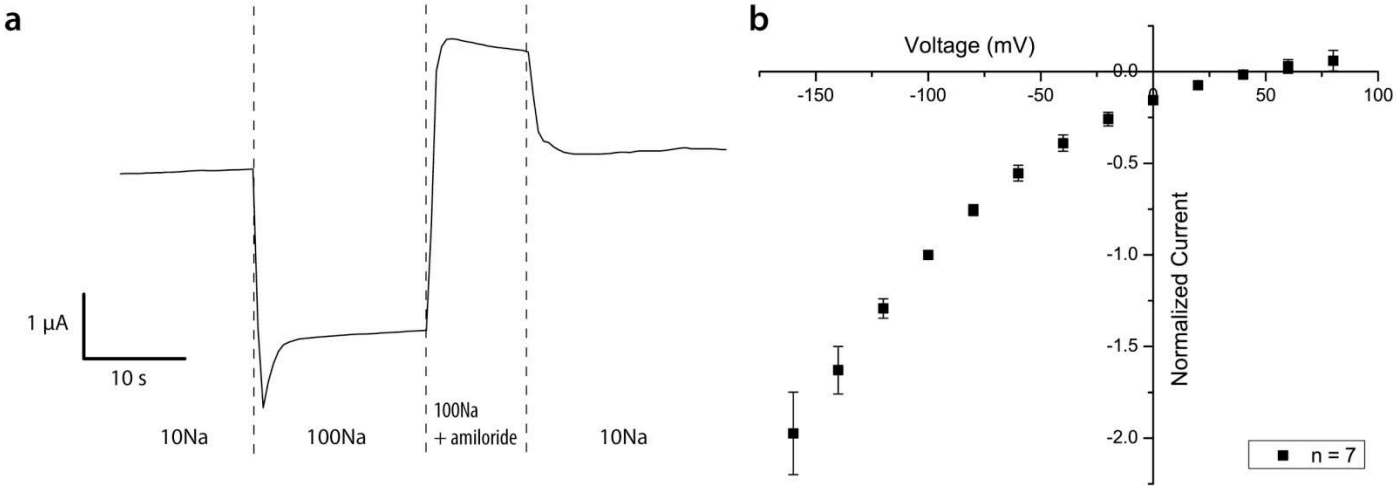

Fig. S5 (a) Real-time TEVC recording of membrane current from a representative oocyte expressing ENaC and voltage clamped to -50 mV. (b) I-V data from ENaC expressing oocytes (n = 7). Amiloride-sensitive currents were normalized to the current at -100 mV and data pooled (mean ± sem).

Influence of pressure variations on the leak conductance

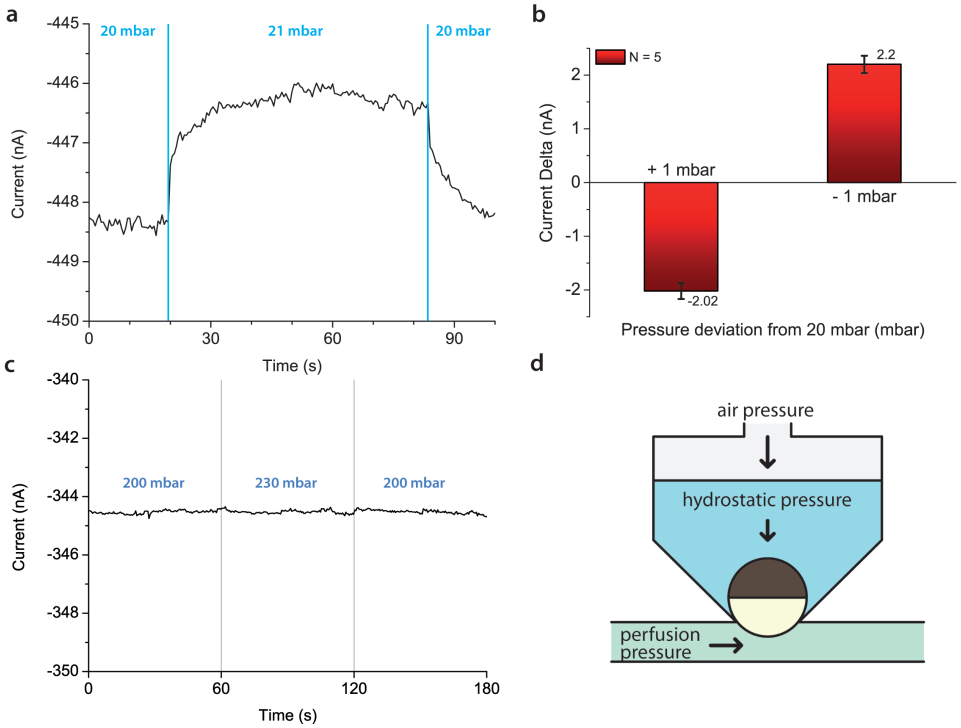

Fig. S6 (a) Time-dependent measurement of leak current varying the air pressure acting on the native oocyte. The transoocyte voltage and the perfusion flow rate were kept constant at -50 mV and 2 µl/s (200 mbar), respectively. (b) Statistical evaluation of 5 oocytes subjected to air pressure variation of 1 mbar in both directions (base pressure 20 mbar). (c) Time-dependent measurement of the leak current varying the perfusion pressure in the microchannel. (d) Scheme showing the direction of the forces (arrows) involved in the experiment.

To study the influence of air pressure variations on the leak conductance a series of experiments were conducted where either the air pressure (Fig. S6a) or the perfusion pressure (Fig. S6c) was varied. These tests demonstrate the system's susceptibility to variations in the immobilization pressure (top pressure) and tolerance to the hydrodynamic resistance of the individual solution pathways. All tests were conducted on native oocytes which have negligible membrane conductance compared to the leak. Therefore, the current resulting from an applied transoocyte voltage is predominantly leak current.